P2.50 **SENSITIVITY TO THE CLOUD MICROPHYSICS SCHEME OF THE SIMULATION OF OROGRAPHIC PRECIPITATION**

J.A. Milbrandt[1,2], M.K. Yau[1], J. Mailhot[2], S. Belair[2]

[1]McGill University, Montreal, Quebec, Canada
[2]Meteorological Services of Canada (MRB-RPN), Dorval, Quebec, Canada

1. INTRODUCTION

There have been considerable increases in computer power in recent years which have allowed for the use of more sophisticated cloud schemes in high-resolution atmospheric models. Consequently, bulk microphysics schemes (BMSs) play an important role in both research and operational numerical weather prediction (NWP) models. Several deficiencies in BMSs have been identified over the past several years. Stoelinga et al. (2003; hereafter S03) list several important issues pertaining to BMSs. Further, bulk schemes vary considerably in their complexity. There is a great variety in the number of hydrometeor categories, the number of prognostic variables per category, the microphysical processes that are included, and the approach to parameterizing each process. It is not immediately obvious which of these aspects are most important. Thus, there is a current need to investigate bulk parameterization methods in order to better design schemes for particular applications.

To address some of these issues in detail, a group of researchers at the University of Washington initiated the aptly named Improvement of Microphysical Parameterization through Observational Verification Experiment (IMPROVE), described in detail in S03. One of the purposes of the experiment was to provide detailed observations for various weather systems with the specific goal of improving quantitative precipitation forecasting (QPF) by mesoscale models using BMSs. The IMPROVE-2 phase of the experiment, the Oregon Cascades Orographic Field Study, was carried out in November-December, 2001. Cases of large-scale weather systems whose precipitation is enhanced by terrain, observed during this phase, are useful since the amount of orographic forcing is essentially known and results in a wide variety of microphysical process, providing a rigorous test for a microphysics scheme.

Corresponding author address:
Dr. Jason A. Milbrandt, 2121 TransCanada Highway, 5th floor, Dorval, QC, H9P 1J3 (Canada); e-mail: jason.milbrandt@ec.gc.ca

During IMPROVE-2, 17 intensive observation periods (IOPs) were carried out. Measurements were made from a variety of remote-sensing and in situ instruments, both ground-based and aircraft-instrumented. The 13-14 December 2001 case had particularly intense precipitation and was well-observed during the IOP. It was the focus of several papers in a special issue (October 2005) of the *Journal of the Atmospheric Sciences*. Due to the availability of published modeling studies and detailed observation for comparison, this case is an excellent candidate for further examination of issues pertaining to bulk microphysics parameterization.

A detailed multi-moment bulk scheme has been recently developed by Milbrandt and Yau (2005a,b). The first major test of the scheme involved the simulation of a supercell hailstorm using a 1-km mesoscale model (Milbrandt and Yau, 2006a,b; hereafter MY06a,b). Although their storm simulations compared favorably to radar observations and the simulated microphysical fields appeared realistic compared to documented observations of similar cases, no in situ microphysical measurements were available and the only surface precipitation quantities were those estimated by the radar. Furthermore, subtleties in the behavior of a microphysics scheme may be masked for a case of deep convection since the forcing is very strong. Further testing of the new scheme on cases of different types of weather and comparison to observed in-cloud microphysical quantities would be useful to provide confidence in the skill of the scheme as a tool for examining parameterization issues.

This study involves high-resolution simulations of the 13-14 December 2001 case using the Milbrandt-Yau BMS. The main objective is to compare simulated precipitation and microphysical fields to observations in order to evaluate the predictive skill of the multi-moment scheme. It shall also be demonstrated that it is possible to produce a very reasonable QPF for this case using the full triple-moment version. We also examine the effects of the number of predicted moments of the hydrometeor size distributions.

2. MODEL DESCRIPTION AND SET-UP

The simulations in this study were performed using the Canadian Mesoscale Compressible Community model, MC2 (version 4.9.8). The MC2 is based on the fully-compressible Euler equations, solved on a Mercator projection, and is a limited-area model capable of one-way self-nesting. The model dynamics are discussed in detail in Benoit et al. (1997). The MC2 uses a comprehensive physics package (Mailhot et al., 1998) which includes a planetary boundary layer scheme based on turbulent kinetic energy, implicit (explicit) vertical (horizontal) diffusion, and a detailed land-surface scheme. The solar and infrared schemes in the radiation package are fully interactive with the model clouds.

Garvert et al. (2005a; hereafter G05), performed simulations of this case using the PSU-NCAR (MM5) mesoscale model. Following the description of their simulations, the MC2 model was initialized at 0000 UTC 13 December 2001 using a gridded analysis from the National Centers for Environmental Prediction–Aviation Model (NCEP-AVN), which was modified to included additional surface and upper-air observations. Boundary conditions were supplied by similar analyses every 6 h for a 36-h simulation. The domain of the 36-km coarse-resolution run was driven by the NCEP-ANV analyses. The model was successively nested to 12-km, 4-km, and 1-km grids.

The 4-km and 1-km control simulations used the triple-moment version of the Milbrandt and Yau (2005a,b; hereafter MY05a,b) BMS. The scheme consists of six hydrometeor variables, two liquid-phase categories – cloud (small, non-sedimenting droplets) and rain (sedimenting drops, including drizzle) – and four frozen-phase categories – ice (pristine crystals), snow (large crystals and aggregates), graupel (medium density rimed-crystals), and hail (high-density graupel and frozen drops). The size distribution of each category is represented by a three-parameter complete gamma function. The full (triple-moment) version of the scheme includes prognostic equations for three moments of the size distributions for each category (except cloud, for which two moments are predicted). The predicted moments are proportional, respectively, to hydrometeor mass content, total number concentration, and reflectivity. Approximately 50 distinct microphysical processes are parameterized. Details of processes and formulations are provided in MY05a and MY05b.

3. CASE DESCRIPTION

The synoptic and mesoscale evolution of the 13-14 December 2001 case are described in detail in G05. The storm was essentially characterized by a large-scale baroclinic system whose precipitation was enhanced by orographic forcing which resulted from strong, lower-tropospheric cross-barrier flow. On 13 December, the frontal system was apparent over the Northern Pacific Ocean. By 0000 UTC 14 December, the surface cyclone had moved inland and a broad cloud shield over a large region near the west coast of North America was present. As the frontal system moved across the Oregon Cascades, several precipitation regimes were observed in the IOP region. Heavy precipitation occurred between approximately 2200 UTC 13 December and 0200 UTC 14 December as a broad rainband ahead of the cold front moved across the area and the cross-barrier (southwesterly) flow at 1-2 km above MSL was 30-40 m s^{-1} causing a significant production of cloud liquid water, allowing for riming to occur at those levels on the wind-ward side of the Cascades. A radar brightband was present at approximately 1.5 km above MSL throughout this period of heavy stratiform precipitation.

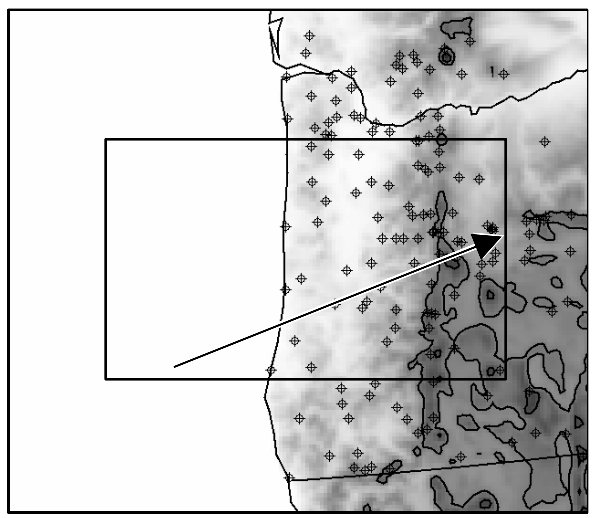

Fig. 1 Orography from 4-km grid (sub-domain only) and location of rain gauges. Dark contour depicts the 1500 m elevation contour. Inner rectangle depicts the 1-km grid. Arrow indicates location of vertical cross-sections in Fig. 5.

4. TRIPLE-MOMENT CONTROL SIMULATION

4.1 *Large-scale Features*

In order to evaluate the BMS in terms of the QPF and microphysical fields by comparison to observations, it is important to verify that the large-scale features simulated by the model were well-simulated. Also, since a major aspect of this study is to follow the modeling strategy of G05 and to compare their MM5 simulations to our MC2 simulations, it is important to ensure that the simulated large-scale variables, which drive the microphysics schemes, are similar enough such that differences in the simulated microphysical fields can be attributed mainly to differences in the BMSs, not difference between the mesoscale models.

The large-scale features of the MC2 simulations were similar to those from satellite observations and the NCEP-AVN analyses. Infrared images (not shown) from GOES at 1200 UTC 13 December, 0000 UTC 14 December, and 1200 UTC 14 December along with the outgoing long-wave radiation (OLR) from the 12-km simulation at the same times. The OLR from the model is strongly dependent on the grid-scale clouds. The model exhibits very similar cloud patterns in terms of location and areal extent for these times, indicating that the regions of large-scale ascent are well-capture by the model.

The geopotential height, winds, and temperature fields at various levels from the coarse-grid (36-km) simulation compare favorably to those fields from the NCEP-AVN analyses (not shown). The differences between the analyses and the MC2 run are similar to those between the analyses and the MM5 simulations of G05. That is, the large-scale features from the MC2 are very similar to those shown in G05 for the same times. This is not surprising since the same set of analyses were used for the initial and boundary conditions for both sets of simulations. It is reassuring, however, to note that difference between the model details do not result in important differences in the fields that drive the microphysics schemes.

4.2 *Mesoscale Features*

Special soundings from the University of Washington, near Cresswell, OR provided measurements upstream of the high terrain in the IOP region. The observed and model soundings at 2100 UTC, 0000 UTC, and 0400 UTC are very similar (not shown). Thus, the upstream temperature and moisture, which are important state variables that drive the microphysics in that region for the high-resolution grids, were well-simulated.

The reflectivity predicted by the microphysics scheme on the 4-km and 1-km grids was compared to radar observations from a radar located in the IOP region. The evolution of the simulated reflectivity was well-captured during the

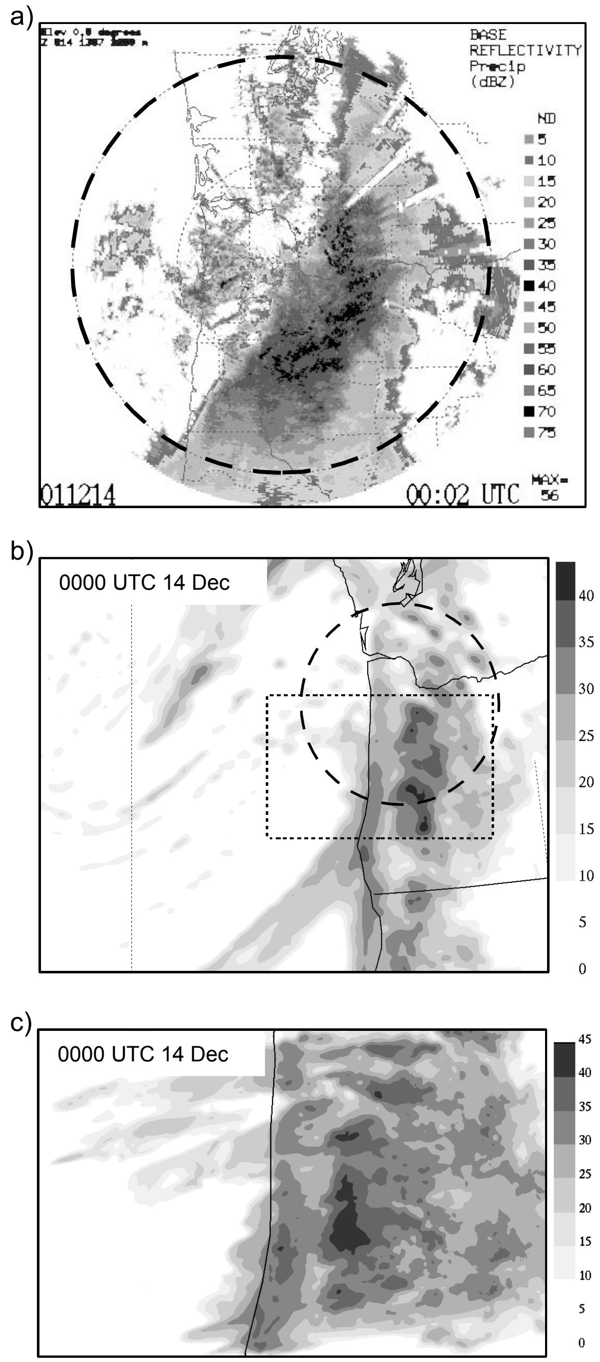

Fig. 2 Reflectivity at 0000 UTC 14 Dec 2001 from a) Portland radar, 0.5º elevation, b) composite from 4-km TM simulation (on full 4-km grid), c) composite from 1-km simulation (on full 1-km grid). Dashed circles depict 200-km range ring for the Portland radar. Inner rectangle in b) depicts 1-km grid.

IOP region, the model reflectivity exhibited similar patterns throughout the periods of pre-frontal showers, heavy stratiform precipitation during the passage of the surface front, and post-frontal showers. An example is shown in Fig. 2 for 0000

UTC, which was approximately mid-way through the period stratiform period. Fig. 2a is a PPI of radar reflectivity at a 0.5º elevation angle from the Portland radar, while Figs. 2b and 2c show the total equivalent reflectivity from the triple-moment scheme from the 4-km and 1-km simulations, respectively. The overall pattern at this time (and others) is similar for the observed and simulated fields, though the 1-km grid naturally has more detail. The maximum reflectivity values are also well-simulated by the model, with small regions with values of 40-45 dBZ from both the radar and model and broader regions with values of 35-40 dBZ.

4.3 *Precipitation*

The most important field resulting from the microphysics scheme is ultimately the precipitation at the surface. Figure 3 shows the 18-h (1400–0800 UTC) accumulated precipitation from the 4-km triple-moment simulation along with rain-gauge values. The shading interval for the model precipitation and the gauges is the same. Thus, darker (lighter) model values under the gauges indicate over-predicted (under-predicted) values while identical shading indicates well–predicted values (correct to within the shading interval). An overall "eyeball" evaluation indicates that the QPF is reasonably good. The model captures the local peak values just inland of the coast, the reduced values in the Willamette Valley (region of lower elevation in Fig. 1), the high values near the crest of the Cascades and the low values in the lee (east) of the mountains. The maximum observed precipitation values just upwind (west) of the mountain crest were underpredicted somewhat by the model. In fact, there is a general under-prediction of precipitation by the model, as indicated by the scatter-plot in Fig. 4a. Note, the scatter-plots in Fig. 4 compare rain gauge values to model values from the nearest grid point. Nevertheless, the general pattern of observed precipitation and the correlation coefficient of 0.73 for model vs. rain-gauge values indicate that the QPF for the triple-moment 4-km run is reasonably good.

The QPF for the triple-moment scheme in the 1-km simulation (not shown) is similar but exhibits greater variability in the regions of complex terrain, corresponding greatly to the high-resolution orography, as expected. However, the scatter-plot for the 1-km run (solid squares in Fig. 4a) and the correlation coefficient of 0.70 do not indicate any improvement in QPF at the higher model resolution. This may simply be a result of an insufficient number of observations in the complex-terrain region of the 1-km grid.

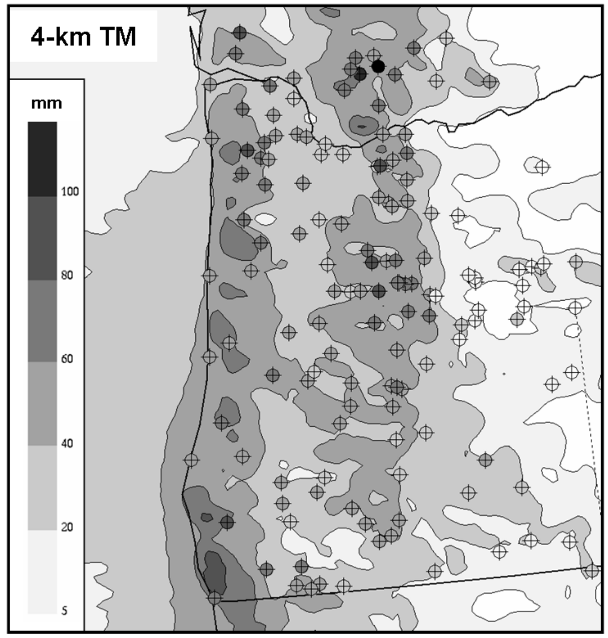

Fig. 3 18-h accumulated precipitation from 1-km TM simulation and rain gauge values. Shading intervals are the same.

5. SENSITIVITY EXPERIMENTS

The simulated reflectivity and precipitation fields from the triple-moment scheme compare favorably to observations. Comparisons (not shown) of in situ measurements from instrumented aircraft during the stratiform period indicated that the simulated microphysical fields were also realistic in terms of hydrometeor type, mass contents, and mean particle sizes. Thus, the BMS appears to be showing considerable skill. This is encouraging for bulk microphysics parameterization. However, the triple-moment scheme, having 17 prognostic variables, is still relatively costly compared to other schemes. This does, however, provide a test-bed to examine issues pertaining to bulk parameterization.

In this section, we examine the sensitivity to the number of prognostic moments for each hydrometeor category. For comparison to the triple-moment control simulations, three sets of sensitivity runs were conducted, each on the 4-km and 1-km grids. One set used the double-moment version (DM) of the Milbrandt-Yau scheme and another used the single-moment version (SM). For further comparison, a third set using a completely different single-moment scheme, that of Kong and Yau (1997) (KY), was also conducted.

5.1 *Precipitation*

The patterns of accumulated precipitation for the DM and SM runs (not shown) are similar overall to the TM runs for both the 4-km (Fig. 3) and 1-km runs. Difference fields reveal that there is little difference between the DM and TM runs, but notable differences in the SM run. This is apparent in the scatter-plots (Fig. 4). There is general under-prediction of precipitation in all of the multi-moment runs with the SM run being slightly worse and with a somewhat greater spread.

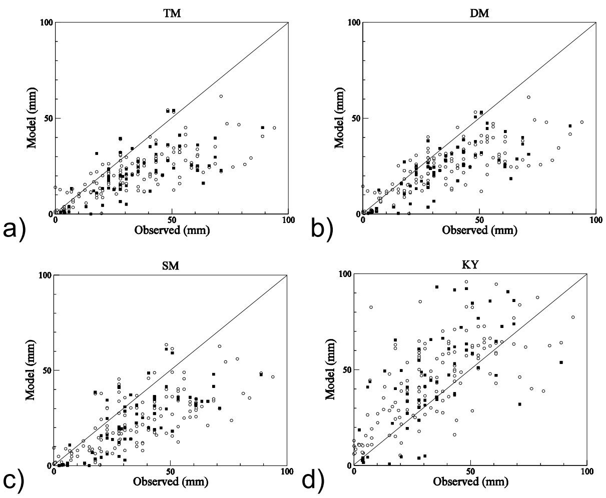

Fig. 4 Scatter-plots of 18-h [1400–0600 UTC] precipitation for rain gauge observations (abscissas) vs. model (ordinates) values. Open (closed) circles are for 4-km (1-km) simulations.

The QPF of from the KY run, however, is much different than all of the runs. As indicated in Fig. 4d, there is a general over-prediction in precipitation and a much lower correlation between observed and simulated values. Much of the over-predicted precipitation in the KY simulations, both at 4-km and 1-km, occurs on the lee side of the Cascades. This is consistent with the simulations of G05, which used a single-moment microphysics scheme similar to KY. That is, the QPF problems for this case described in G05 have been essentially reproduced in our KY simulations but notably improved in the simulations with all versions of the multi-moment scheme.

5.2 *Hydrometeor Fields*

The differences in simulated precipitation between the multi-moment runs and the KY runs appear to be partly related to the way the ice-phase spectrum is partitioned and treated. Figure 5 depicts, for the 1-km simulations, vertical cross-sections (see arrow in Fig. 1 for location) of the time-averaged (2200-0200 UTC) mass contents of snow (thin contours), graupel (thick contours), rain (dashed), and cloud water (shading). For clarity, pristine ice and ice pellets (hail) are excluded from the figures for the multi-moment runs. The large rain content on the lee of the Cascades for the KY runs corresponds to the excess QPF in that area. As can be partly inferred from the figure, that rain originates from the large snow content aloft which is advected over the mountains by the strong cross-barrier winds, descend rapidly in the downdraft on the lee side, falls through 0ºC isotherm into warm air, and melts. Despite the

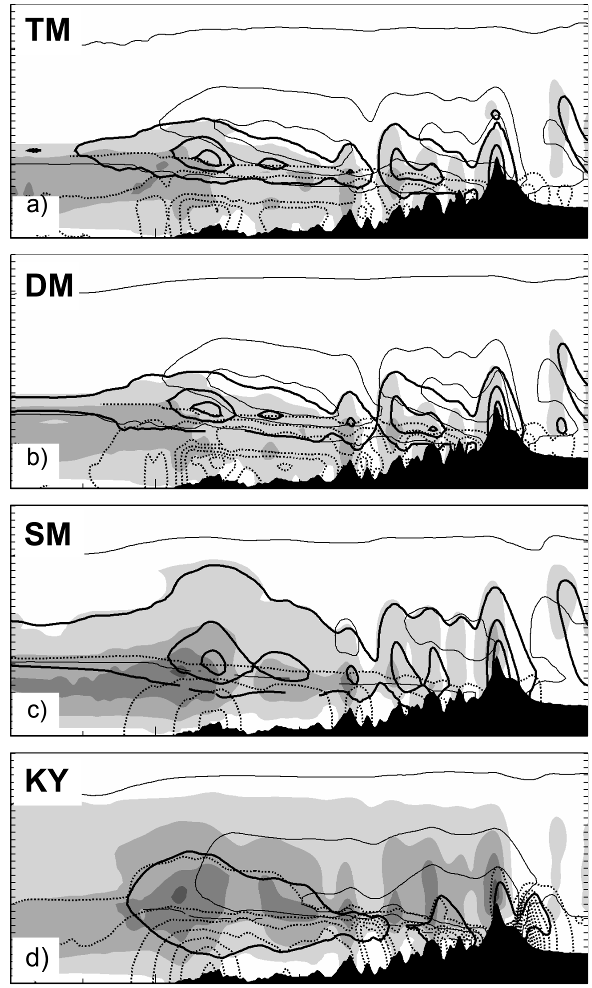

Fig. 5 Vertical cross-sections (from 1000–200 hPa) of time-averaged (2200–0200 UTC) hydrometeor mass contents from 1-km simulations for a) TM, b) DM, c) SM, and d) KY. Shading, thin, thick, and dashed contours are for, respectively, cloud, snow, graupel, rain. Shading/contours indicate, respectively: 0.01, 0.2, 0.4...; 0.01, 0.5, 1.0…; 0.01, 0.2, 0.4,…; and 0.01, 0.2, 0.4,… g m^{-3}.

fact that the snow contents in the multi-moment runs are similar to that of KY (though they are somewhat less for SM), there is considerably more conversion to graupel for those runs as snow undergoes riming in the presence of cloud water. The graupel sediments more quickly than snow and therefore precipitates sooner, on the windward side of and in the vicinity of the mountain peaks. This hypothesis was put forth in G05 to explain the excess precipitation on the lee side in their simulations and is consistent with our results.

5. CONCLUSION

The 13-14 December 2001 IMPROVE-2 case has proven to be an excellent testing ground for further examination and evaluation of the Milbrandt-Yau multi-moment BMS. Comparison to radar, rain gauges, and in situ microphysical measurements indicated that the full triple-moment version of the scheme performed very well for the simulation of this case of orographically enhanced precipitation. This is encouraging for bulk microphysics parameterization since it indicates that it is possible for a BMS to simulate with skill a complex variety of microphysical processes. This case study provides confidence that the multi-moment scheme can be used for detailed process studies using 3D mesoscale or cloud-resolving models and for continuing to examine parameterization issues pertaining to bulk schemes.

It appears that for this case, differences in the formulations of the six-hydrometeor-category (4-ice) single-moment version of the Milbrandt-Yau scheme and the four-category (2-ice) Kong-Yau scheme are of greater importance to the QPF than the number of moments predicted. This result is different from that of MY06b, which showed that for a case of deep convection there were large differences between simulations with the single-moment version and the double-moment version of the scheme. Further examination both of differences between BMSs and of the importance of the number of prognostic moments, and for which hydrometeor categories, is thus warranted.

REFERENCES

Benoit, R., J.M. Desgagné, P. Pellerin, S. Pellerin, Y. Chartier, and S. Desjardins, 1997: The Canadian MC2: A semi-Lagrangian, semi-implicit wideband atmospheric model suited for finescale process studies and simulation. *Mon. Wea. Rev.*, **125**, 2382-2415.

Garvert. M.F., B.A. Colle, and C.F. Mass, 2005a: The 13-14 December 2001 IMPROVE-2 event. Part I: Synoptic and mesoscale evolution and comparison with a mesoscale model simulation. *J. Atmos. Sci.*, **62**, 3474-3492.

Kong, F. and M.K. Yau, 1997: An explicit approach to microphysics in MC2. *Atm. Ocean.* **33**, 257-291.

Mailhot, J., and Coauthors, 1998: Scientific description of RPN physics library – Version 3.6. Atmospheric Environment Service Tech. Rep. v 3.6, 188 pp.

Milbrandt, J.A. and M.K. Yau, 2005a: A multimoment bulk microphysics parameterization. Part I: Analysis of the role of the spectral shape parameter. *J. Atmos., Sci.*, **62**, 3051-3064.

Milbrandt, J.A. and M.K. Yau, 2005b: A multimoment bulk microphysics parameterization. Part II: A proposed three-moment closure and scheme description. *J. Atmos., Sci.*, **62**, 3065-3081.

Milbrandt, J.A. and M.K. Yau, 2006a: A multimoment bulk microphysics parameterization. Part III: Control simulation of a hailstorm. *J. Atmos. Sci.* In press.

Milbrandt, J.A. and M.K. Yau, 2006a: A multimoment bulk microphysics parameterization. Part IV: Sensitivity tests. *J. Atmos. Sci.* In press.

Stoelinga, M.T. and Coauthors, 2003: Improvement of Microphysical Parameterization through Observational Verification Experiment. *Bull. Amer. Meteor. Soc.*, **84**, 1807-1826.